

Crystallization of Mannitol below T_g' during Freeze-Drying in Binary and Ternary Aqueous Systems

Abira Pyne,^{1,2} Rahul Surana,¹ and Raj Suryanarayanan^{1,3}

Received February 19, 2002; accepted February 28, 2002

Purpose. To characterize the phase transitions in a multicomponent system during the various stages of the freeze-drying process and to evaluate the crystallization behavior below T_g' (glass transition temperature of maximally freeze-concentrated amorphous phase) in frozen aqueous solutions and during freeze-drying.

Methods. X-ray powder diffractometry (XRD) and differential scanning calorimetry (DSC) were used to study frozen aqueous solutions of mannitol with or without trehalose. By attaching a vacuum pump to the low-temperature stage of the diffractometer, it was possible to simulate the freeze-drying process *in situ* in the sample chamber of the XRD. This enabled real-time monitoring of the solid state of the solutes during the process.

Results. In rapidly cooled aqueous solutions containing only mannitol (10% w/w), the solute was retained amorphous. Annealing of frozen solutions or primary drying, both below T_g' , resulted in crystallization of mannitol hydrate. Similar effects were observed in the presence of trehalose (2% w/w). At higher concentrations ($\geq 5\%$ w/w) of this noncrystallizing sugar, annealing below T_g' led to nucleation but not crystallization. However, during primary drying, crystallization of mannitol hydrate was observed.

Conclusions. The combination of *in situ* XRD and DSC has given a unique insight into phase transitions during freeze-drying as a function of processing conditions and formulation variables. In the presence of trehalose, mannitol crystallization was inhibited in frozen solutions but not during primary drying.

KEY WORDS: annealing; differential scanning calorimetry; frozen; mannitol; trehalose; X-ray powder diffractometry.

INTRODUCTION

Mannitol, a nonreducing sugar, is a commonly used excipient in freeze-dried pharmaceutical formulations. It crystallizes readily when its aqueous solutions are freeze-dried (1). Known for its excellent cake-forming properties, mannitol is frequently used as a bulking agent in freeze-dried protein formulations. These formulations may contain, in addition to the active ingredient, a stabilizer (lyoprotectant), a bulking agent, buffer salts, and a surfactant.

The first step in the freeze-drying process is the cooling of aqueous solutions of the formulation ingredients. For the sake of simplicity, let us consider a solution containing one solute. If the solute does not crystallize, the frozen system is

characterized by the glass transition temperature of the maximally freeze-concentrated solute, T_g' . If the solute crystallizes and forms a eutectic with ice, the eutectic temperature, T_e , is of significance. The T_g' and T_e govern the selection of the primary drying temperature. Primary drying above T_g' leads to the collapse of the freeze-dried cake whereas drying above the eutectic temperature can result in "melt-back." Both the collapse and the melt-back of the lyophile result in a pharmaceutically inelegant and unacceptable product. For example, a loss in the strength of the cake structure, stickiness, and discoloration are some of the undesirable attributes of a collapsed lyophile.

Though mannitol predominantly exists in the crystalline state in lyophiles, retaining it amorphous may confer several advantages. It can then serve as a lyoprotectant (2). When compared with sucrose, a popular lyoprotectant, mannitol can be used over a wider pH range (3). Moreover, vial breakage, attributed to crystallization of mannitol during freeze-drying, may be prevented by retaining mannitol amorphous (4,5). Mannitol crystallization may be inhibited by rapidly cooling mannitol solutions, primary drying at low temperatures, or the presence of additives (1,6,7). Because the crystallization behavior of mannitol is significantly influenced by additives, this is worthy of detailed investigation.

However, there are situations where it is desirable to have crystalline mannitol in a freeze-dried product. Crystallization of mannitol results in an elegant cake. Moreover, if mannitol crystallizes in frozen aqueous solutions, primary drying can be carried out at a temperature substantially higher than T_g' . To maximize crystallization of mannitol, thermal treatment is usually recommended. Annealing is an isothermal step that is often incorporated in freeze-drying cycles (8). It is usually conducted above the T_g' to facilitate maximum solute crystallization in frozen aqueous solutions (9). Processing or storage below T_g' is believed to decelerate if not prevent the crystallization of solutes.

Trehalose has recently been approved by the U.S. Food and Drug Administration for use in parenteral formulations (10). It remains amorphous during freeze-drying and serves as a lyoprotectant. To accelerate drying and also to obtain a pharmaceutically elegant lyophile with structural integrity, a crystalline bulking agent can be combined with a lyoprotectant. In these systems, it is advisable to ensure that the bulking agent is in a crystalline form before primary drying is initiated. This not only enables primary drying to be carried out at a higher temperature, but also shortens the secondary drying cycle (11). Under certain circumstances, the bulking agent may not have crystallized completely even at the end of freeze-drying. If there is crystallization during storage, this will be accompanied by the release of water associated with the amorphous phase (12). The interaction of the released water with the amorphous formulation ingredients can result in detrimental physical and chemical changes. If the active ingredient is a protein, the crystallization of the stabilizing excipient could lead to loss of lyoprotection (8).

Numerous investigations deal with the solid-state behavior of mannitol in frozen and freeze-dried systems (1,6,7,13). We had previously investigated the effect of cooling rate and the influence of phosphate buffers and polyvinylpyrrolidone (PVP) on the crystallization behavior of mannitol in frozen

¹ Department of Pharmaceutics, University of Minnesota, 308 Harvard St. S.E., Minneapolis, Minnesota 55455.

² Current address: Eli Lilly & Company, Lilly Corporate Center, Indianapolis, Indiana 46285.

³ To whom correspondence should be addressed. (e-mail: surya001@tc.umn.edu)

aqueous solutions (14). The crystallization of mannitol in the frozen solution may only be prevented by carefully controlling the processing conditions and through the use of additives. For example, mannitol was retained amorphous only when its aqueous solution was rapidly cooled and maintained at temperatures less than T_g' . However, when the system was heated past its T_g' , there was rapid solute crystallization. In fact, the crystallization was initiated even before the glass transition was complete. This is not surprising given that mannitol is invariably crystalline in freeze-dried formulations.

It is now well recognized that there may be sufficient molecular mobility below the glass transition temperature to cause crystallization (15). In light of the strong tendency of mannitol to crystallize, it is conceivable that crystallization may occur even below T_g' . Interestingly, there are no literature reports on the physical stability of glassy mannitol in frozen aqueous solutions. If amorphous mannitol is desired, it is particularly important to characterize these systems at temperatures less than T_g' . If mannitol crystallizes under these conditions, it is pertinent to study the crystallization kinetics as a function of temperature. As mentioned previously, trehalose, a lyoprotectant, may be present along with mannitol in freeze-dried formulations. Therefore, the crystallization behavior of mannitol in presence of trehalose is also of relevance.

Our first objective was to characterize frozen mannitol solutions during and after annealing under several conditions. The crystallization kinetics were studied both by X-ray powder diffractometry (XRD) and differential scanning calorimetry (DSC). Our second objective was to determine the influence of trehalose, which is a noncrystallizing solute, on the crystallization behavior of mannitol during the various stages of freeze-drying.

MATERIALS AND METHODS

Materials

D-Mannitol ($C_6H_{14}O_6$, Sigma, St. Louis, Missouri) and D(+) trehalose dihydrate ($C_{12}H_{22}O_{11} \cdot 2H_2O$, Sigma) were used as received.

Methods

Differential Scanning Calorimetry

A differential scanning calorimeter (Model 2920, TA Instruments, New Castle, Delaware) equipped with a refrigerated cooling system was used. It was calibrated using indium, mercury, and distilled water as standards. About 10–15 mg of each solution was weighed in an aluminum pan and hermetically sealed. Aqueous solution of mannitol was cooled to -60°C at $20^\circ\text{C}/\text{min}$ and held for 20 min. It was then heated to a chosen temperature below the observed glass transition temperatures (unless otherwise mentioned) at $5^\circ\text{C}/\text{min}$ and held for a predetermined time period before it was cooled back to -60°C . The system was then reheated to room temperature at $5^\circ\text{C}/\text{min}$. In the case of solutions containing mannitol and trehalose, the cooling rate was $10^\circ\text{C}/\text{min}$. All the DSC curves presented (Figs. 2, 5, and 6) are the second heating scans. Annealing at temperatures below both the ob-

served transitions has been referred to as “sub- T_g' annealing.”

X-Ray Powder Diffractometry

An X-ray powder diffractometer (Model XDS 2000, Scintag, Cupertino, California) with a variable temperature stage (Micristar, Model 828D, R.G. Hansen & Associates, Santa Barbara, California; working temperature range of -190°C to $+300^\circ\text{C}$) was used. The temperature stage of the X-ray diffractometer was attached to a vacuum pump. As a result, it was possible to carry out the entire freeze-drying process in the sample chamber of the X-ray diffractometer. An accurately weighed amount of solution (~ 100 mg) was filled into a copper sample holder and cooled at a constant predetermined rate from room temperature to -50°C . It was held for 20 min and heated to the annealing or primary drying temperature at $5^\circ\text{C}/\text{min}$. The experimental conditions were different when systems containing mannitol and trehalose were investigated. The specific details are provided below in the “Results and Discussion” section.

XRD patterns were obtained by exposing the sample to Cu K_α radiation ($45 \text{ kV} \times 40 \text{ mA}$), wherein the scanning speed was $5^\circ 2\theta \text{ min}^{-1}$ and the step size was $0.03^\circ 2\theta$. During the XRD runs, the sample was maintained under isothermal conditions at the selected temperatures. The frozen solution was then subjected to primary drying *in situ* in the sample chamber of the X-ray diffractometer. The pressure was ~ 100 mtorr. The primary drying was carried out until all the crystalline ice was removed. The sample was then heated to the secondary drying temperature (-10°C) where the drying was continued for the desired time period.

RESULTS AND DISCUSSION

Characterization of Mannitol

The “as is” mannitol was characterized by XRD and DSC. The XRD pattern of mannitol matched that of the anhydrous β -polymorph reported in the literature (16). When heated in the differential scanning calorimeter it melted at $\sim 165^\circ\text{C}$, which was close to the reported melting temperature of 166.5°C (16).

Frozen Aqueous Solutions of Mannitol

The solute was retained amorphous when an aqueous solution of mannitol was cooled at $20^\circ\text{C}/\text{min}$ in the differential scanning calorimeter. However, there was partial crystallization of mannitol at slower cooling rates of $10^\circ\text{C}/\text{min}$ or $5^\circ\text{C}/\text{min}$ (14). In contrast, low-temperature XRD studies did not reveal any crystallization when cooled at $10^\circ\text{C}/\text{min}$ or at $5^\circ\text{C}/\text{min}$, suggesting that the crystalline mannitol concentration was below the detection limit of XRD.

When an aqueous mannitol solution was cooled to -60°C at $20^\circ\text{C}/\text{min}$ and then heated, several thermal events were observed (Fig. 1): two glass transitions with onset at approximately -32°C ($T_{g'1}$) and approximately -25°C ($T_{g'2}$); an exotherm attributable to solute crystallization with an onset at approximately -22°C ; and an endotherm due to eutectic melting of mannitol and ice. These transitions were explained in a preceding manuscript (14). Multiple glass transitions in frozen aqueous solutions, while still incompletely understood, have been the subject of several discussions (e.g., Refs. 17–19).

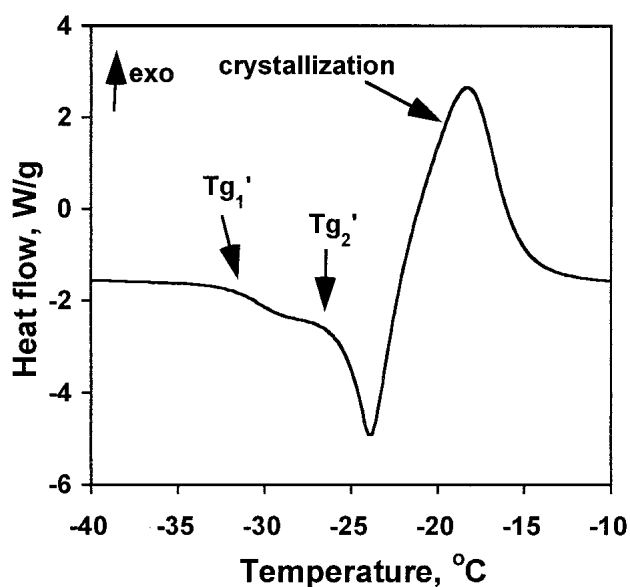


Fig. 1. DSC heating profile of frozen aqueous solution of mannitol (10% w/w). The solution was cooled from room temperature to -60°C at $20^{\circ}\text{C}/\text{min}$. It was held at -60°C for 20 min and heated to room temperature at $5^{\circ}\text{C}/\text{min}$.

The stability of an amorphous freeze-concentrate is usually dictated by the molecular mobility of the system. This is expected to be reduced below the glass transition temperature of the amorphous freeze-concentrate, where the system is "frozen" in a glassy matrix. This glass transition temperature will be significantly influenced by the amount of unfrozen water in the system.

Because mannitol has a strong tendency to crystallize, we decided to examine in detail the physical stability of the amorphous freeze-concentrate below both the glass transitions. To understand the dynamics of the glassy mannitol in the freeze-concentrate, it was annealed at -33°C (i.e., below $T_g'1$) for various time periods, cooled to -60°C , and heated to room temperature at $5^{\circ}\text{C}/\text{min}$ (Fig. 2). There was a progressive decrease in the enthalpy of crystallization as a function of the annealing time. This strongly suggests that mannitol crystallized during sub- T_g' annealing. From Fig. 2, it is also evident that the onset temperature for crystallization decreased as a function of the annealing time. If mannitol crystallizes during annealing, the crystalline mannitol concentration will increase as a function of the annealing time. This crystalline phase will facilitate further crystallization of mannitol, which is reflected in the decrease in the onset temperature of crystallization. Similar annealing experiments were performed at -35 , -37 , and -39°C (DSC curves not shown). For a given annealing time, as the annealing temperature increased (i.e., closer to $T_g'1$), the enthalpy of crystallization decreased. This indicated that the extent of crystallization during annealing increased as a function of the annealing temperature.

Annealing also seemed to cause the merger of the two transitions, resulting in a single glass transition. The longer the annealing, the higher was this temperature. However, these results should be viewed with caution. With annealing, there is a progressive increase in the crystalline mannitol content and a consequent decrease in the amorphous content. Therefore, the glass transition signal may become weak and may not be readily detectable.

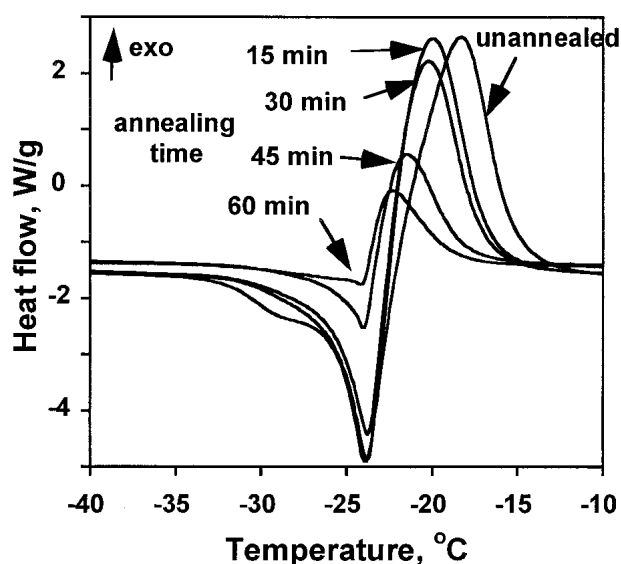


Fig. 2. DSC heating profiles of frozen aqueous solutions of mannitol which had been annealed at -33°C for time periods ranging from 0 to 60 min. Aqueous mannitol (10% w/w) solution was cooled from room temperature to -60°C at $20^{\circ}\text{C}/\text{min}$ and held for 20 min. The solution was then heated to the annealing temperature of -33°C at $5^{\circ}\text{C}/\text{min}$, annealed, cooled to -50°C at $20^{\circ}\text{C}/\text{min}$, and reheated at $5^{\circ}\text{C}/\text{min}$ (second heating). The second heating scans are presented.

Low-temperature XRD provided direct evidence of mannitol crystallization below $T_g'1$. When the solution was annealed at -33°C , characteristic peaks of mannitol hydrate (e.g., at 9.1 , 18 , and $21^{\circ}2\theta$) were observed (Fig. 3). Similar results were obtained when the solutions were annealed at -35 , -37 and -39°C (results not shown). At each of these temperatures, the sum of the integrated intensities of mannitol hydrate peaks, over the angular range of 16 to $19^{\circ}2\theta$, were plotted as a function of the annealing time (Fig. 4a). An in-

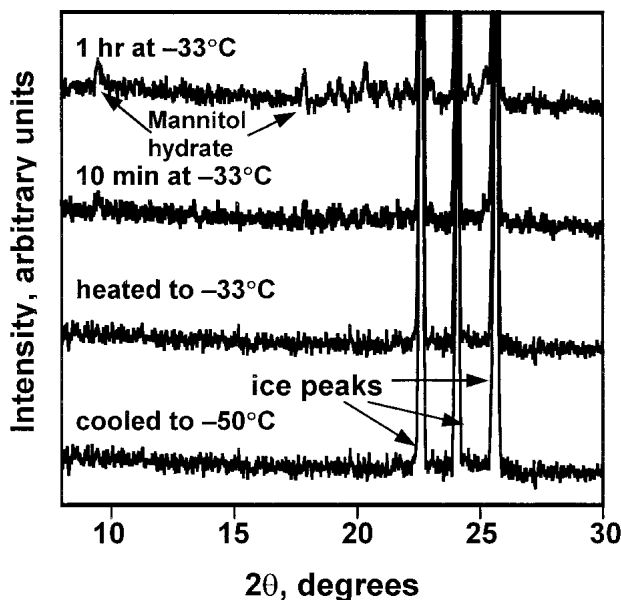


Fig. 3. XRD patterns obtained during annealing of frozen aqueous solutions of mannitol at -33°C . Mannitol solution (10% w/w) was cooled from room temperature to -50°C , heated to -33°C at $5^{\circ}\text{C}/\text{min}$, and annealed for 60 min.

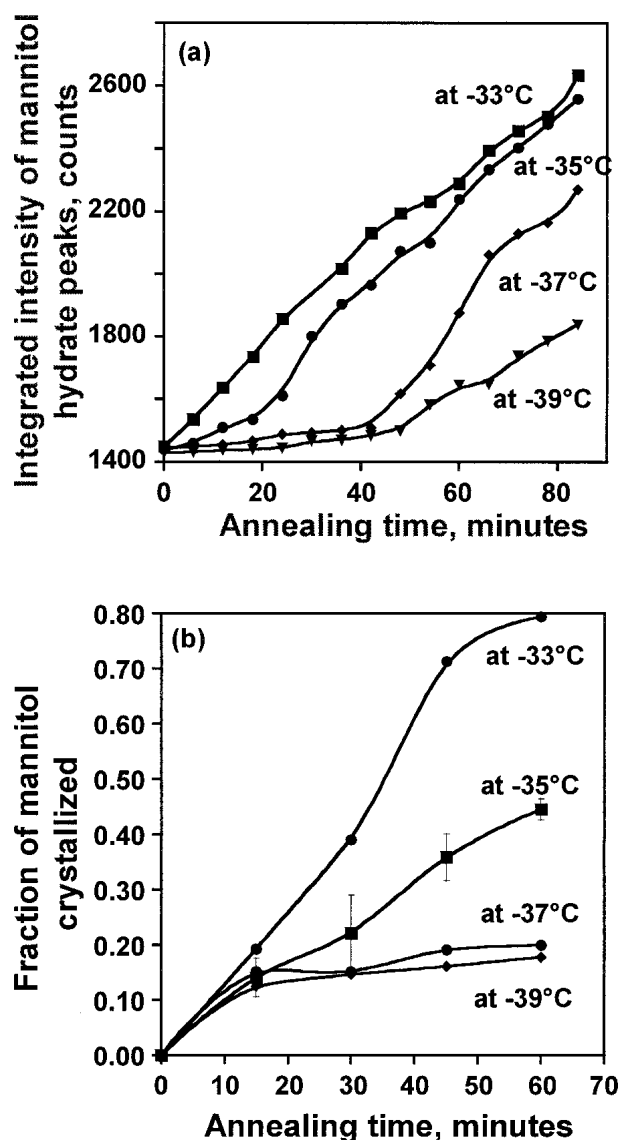


Fig. 4. Kinetics of mannitol crystallization as a function of annealing temperature and time. (a) Isothermal crystallization of mannitol during sub- T_g' annealing in the X-ray powder diffractometer. (b) Fraction of mannitol crystallizing in the differential scanning calorimeter as a function of annealing time and temperature. Error bars represent standard deviations of selected samples ($n = 3$).

crease in the annealing temperature resulted in an increase in the crystalline mannitol hydrate content. At the higher annealing temperatures (-33 and -35°C) there appeared to be no lag time whereas at the lower temperatures (-37 and -39°C), crystalline mannitol hydrate was detected only after annealing for ~ 45 min. Once crystallization was evident, there was a progressive increase in the intensities of mannitol hydrate peaks as a function of the annealing time. Under all annealing conditions, even after annealing for over 80 min, the crystallization appeared to be substantially incomplete. This conclusion is based on the observation that an increase in the annealing temperature caused an increase in the crystallinity of mannitol hydrate (annealing temperatures $\geq T_g'_2$).

The enthalpy of crystallization, determined by DSC, was also used to study the kinetics of mannitol hydrate crystallization (Fig. 4b). The fraction of amorphous solute at each

annealing time was obtained by dividing the enthalpy of crystallization of that sample by that of the unannealed sample. The remainder of the solute was assumed to be in the crystalline state. This calculation assumes that the unannealed sample, when heated past $T_g'_2$, will crystallize completely. The DSC and XRD results are qualitatively similar. In the X-ray diffractometer, crystallization occurred under isothermal conditions whereas the enthalpy of crystallization in the differential scanning calorimeter was obtained by subjecting the sample to a controlled temperature program. When the annealing was carried out several degrees below $T_g'_1$ (at -37 and -39°C), the fraction of mannitol that crystallized was low.

Frozen Aqueous Solutions of Mannitol and Trehalose

Noncrystallizing cosolutes including sucrose, trehalose, and proteins can significantly influence the crystallization behavior of mannitol (1,20). When freeze-dried in presence of trehalose, mannitol is retained amorphous when the trehalose to mannitol ratio $\geq 7:3$ (w/w). Trehalose has excellent lyoprotectant activity and has been used as a stabilizer in numerous protein formulations. It was therefore of interest to study the effect of lower concentrations of trehalose on mannitol crystallization.

The DSC curve of the frozen aqueous solution containing mannitol (10% w/w) and trehalose (5% w/w) revealed two glass transition events ($T_g'_1$ and $T_g'_2$) with onset temperatures of -41°C and -33°C , respectively (Fig. 5, unannealed sample). The glass transitions were followed by a mannitol hydrate crystallization exotherm and an endotherm (not completely shown) attributed to overlapping eutectic and ice-melting events.

We had earlier seen (Fig. 1) that the $T_g'_1$ and $T_g'_2$ of mannitol were approximately -32°C and approximately -25°C , respectively. When an aqueous solution of trehalose (5% w/w) was subjected to DSC studies under similar condi-

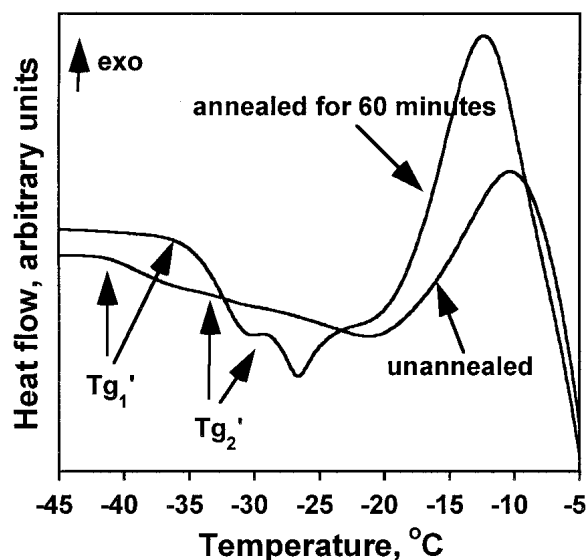


Fig. 5. The effect of sub- T_g' annealing (at -41°C) in frozen aqueous solutions containing mannitol (10% w/w) and trehalose (5% w/w). The solutions were cooled from room temperature to -60°C at $10^\circ\text{C}/\text{min}$, heated to -41°C , annealed for 60 min, cooled to -60°C , and reheated at $5^\circ\text{C}/\text{min}$. The second heating scan has been overlaid on the DSC heating profile of the unannealed sample.

tions, glass transition events were observed at -45 and -31°C (not shown). Therefore, the $T_{g'1}$ of the trehalose-mannitol mixture (-41°C) occurred between the $T_{g'1}$ values of the individual components (-32 and -45°C). However, the $T_{g'2}$ of the mixture (-33°C) was found to be lower than the $T_{g'2}$ of mannitol (-25°C) and trehalose (-31°C). It has been shown that the glass transition temperature of frozen aqueous solutions containing mannitol and sucrose ($\sim -40^\circ\text{C}$) was lower than that of mannitol ($\sim -32^\circ\text{C}$) and sucrose ($\sim -33^\circ\text{C}$) (6). This can be attributed to the higher concentration of unfrozen water in the mixture than in the frozen solutions containing only the individual components.

The next objective was to determine the effect of sub- T_g' annealing at several temperatures ranging from -41 to -49°C . Figure 5 is a representative example. Sub- T_g' annealing caused a pronounced change in the DSC profiles, and the onset of the first glass transition occurred at a higher temperature of approximately -39°C . A clearer $T_{g'2}$ was observed at approximately -27°C with associated enthalpic recovery (Fig. 5, annealed sample). Significantly, mannitol crystallization occurred at a lower temperature, and the enthalpy of crystallization was much higher than that of the unannealed sample.

We believe that when aqueous solutions of mannitol and trehalose were cooled, neither of the solutes crystallized. As mentioned earlier, trehalose is expected to remain amorphous. It appears to have inhibited ice crystallization, thereby preventing the formation of a supersaturated solution of mannitol, a condition necessary for crystallization (21,22). Because annealing below T_g' facilitates ice crystallization (19,23), it will result in supersaturation of mannitol, followed by its nucleation. The presence of nuclei in the annealed sample is likely to be responsible for the sharper crystallization exotherm at a lower temperature and for the increase in the enthalpy of crystallization of mannitol (compare the DSC curves of the unannealed and annealed samples in Fig. 5). Similar observations were made when the cooling rates employed were reduced to $0.5^\circ\text{C}/\text{min}$ or the annealing times were increased to 8 h. Therefore, neither slower cooling nor prolonged annealing caused the crystallization of mannitol below $T_{g'1}$.

The two glass transitions of the annealed solution (~ -39 and -27°C after annealing for 60 min) were higher than that of the unannealed sample (-41 and -33°C). This is an indirect proof that annealing resulted in ice crystallization, decreased the unfrozen water content in the amorphous freeze-concentrate, and increased the glass transition temperatures. Ice crystallization appears to have been followed by the nucleation but not the crystallization of mannitol.⁴ This was evident from low-temperature XRD of these systems (results not shown). Aqueous solutions of mannitol (10% w/w) and trehalose (5% w/w) were cooled from room temperature to -60°C at $10^\circ\text{C}/\text{min}$, heated to -45°C at $5^\circ\text{C}/\text{min}$, annealed

for 0, 30, or 60 min, cooled to -60°C , and heated at $5^\circ\text{C}/\text{min}$ to -25°C and the XRD pattern was obtained. There was no crystallization of mannitol in the unannealed solution. XRD patterns, obtained during annealing, did not reveal any crystallization at -45°C . The characteristic peak of mannitol hydrate at $9.1^\circ 2\theta$ was first seen only after annealing at -45°C for 30 min and heating to -25°C . The peak was pronounced and readily discernable when the annealing time was increased to 60 min (data not shown). The choice of -25°C for obtaining the isothermal XRD scan of the annealed sample was based on the DSC profiles of the annealed and unannealed systems (Fig. 5). From Fig. 5 it is evident that the onset of crystallization occurs only at temperatures higher than -25°C .

The effect of annealing temperature over the range -37 to -49°C was next investigated (Fig. 6). A decrease in annealing temperature from -37 to -45°C lowered the crystallization onset temperature and increased the enthalpy of crystallization. On annealing at temperatures $< -45^\circ\text{C}$, the enthalpy of crystallization decreased. The lowest crystallization onset and the maximum enthalpy of crystallization were observed following annealing at -45°C (Fig. 6a), strongly suggesting

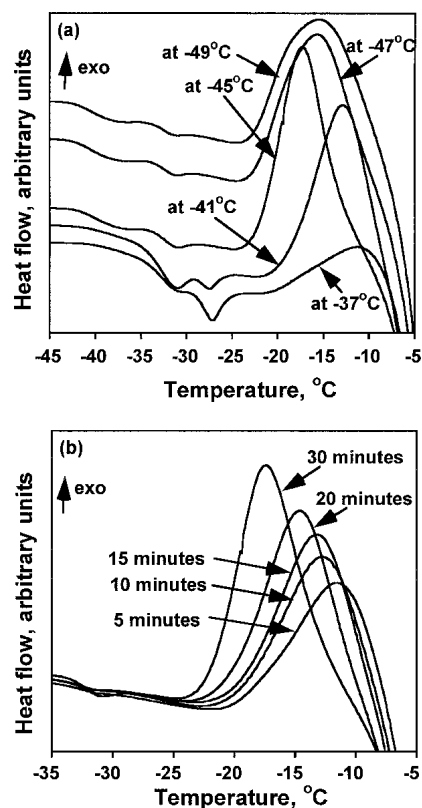


Fig. 6. (a) The effect of annealing temperature on the crystallization behavior of mannitol in frozen aqueous solutions containing mannitol (10% w/w) and trehalose (5% w/w). The solutions were cooled from room temperature to -60°C at $10^\circ\text{C}/\text{min}$, heated to the annealing temperature (-49 , -47 , -45 , -41 or -37°C) at $5^\circ\text{C}/\text{min}$, annealed for 30 min, cooled to -60°C , and reheated at $5^\circ\text{C}/\text{min}$. The second heating scans are shown here. (b) The effect of annealing time on the crystallization behavior of mannitol in frozen aqueous solutions containing mannitol (10% w/w) and trehalose (5% w/w). The solutions were cooled from room temperature to -60°C at $10^\circ\text{C}/\text{min}$, heated to -45°C at $5^\circ\text{C}/\text{min}$, annealed for 5 to 30 min, cooled to -60°C , and reheated at $5^\circ\text{C}/\text{min}$. The second heating scans are shown here.

⁴ These effects were very clear when the system was annealed at -45°C for longer periods of time. With an increase in annealing time, the T_g s of the system merged to give rise to a single glass transition event. For example, the second heating scan of a sample annealed at -45°C for 8 h showed only one $T_{g'}$ at -33.5°C . The enthalpy of crystallization was at least 50% higher than that of the unannealed sample. Annealing for these prolonged periods also did not lead to crystallization below the $T_{g'}$.

that maximum nucleation occurred at this temperature. Thus, the nucleation rate seemed to reach a maximum when annealing was carried out a few degrees below Tg'_1 of -41°C .

Annealing at -45°C was studied in greater detail. As the annealing time increased, the crystallization exotherm was observed at a lower temperature (Fig. 6b). The enthalpy of crystallization also exhibited a pronounced increase as a function of the annealing time. We propose that annealing led to nucleation and the number of nuclei increased as a function of the annealing time. As the number of nuclei increased, crystallization on heating occurred at a lower temperature and a larger fraction of the amorphous mannitol crystallized. These results strongly suggest nucleation of mannitol during annealing. The other thermal events observed between -40 and -25°C (Fig. 6a) were discussed in a recent presentation and are the subject of a manuscript in preparation (24).

The nucleation behavior of mannitol detailed above has interesting similarities with that of aqueous solutions of citric acid (25). The rate of nucleation, J , decreased with an increase in degree of supersaturation, S . According to the classical homogeneous nucleation theory, J increases as a function of S [Eq. (1)]. However, the associated increase in viscosity may negate this effect resulting in a decrease in nucleation rate (25,26).

$$J = A \exp\left[-\frac{16 \pi \sigma^3 v^3 N}{3 R^3 T^3 (\ln S)}\right] \quad (1)$$

Here, A is the collision factor, v is the molecular volume of the embryo, σ is the interfacial energy, N is Avogadro's number, R is the gas constant, and T is the absolute temperature. As proposed by Turnbull and Fisher (26), the dependence of J on the viscosity is given by

$$J = A' \exp\left(\frac{-\Delta G^* - \Delta G_a}{kT}\right) \quad (2)$$

where A' is a pre-exponential factor, ΔG^* is the Gibb's free energy for the formation of clusters, ΔG_a is the activation energy for transport across the nucleus-liquid interface or the activation energy for diffusion, and k is the Boltzmann constant. With an increase in viscosity, ΔG_a increases and there will be a decrease in the nucleation rate. Similar behavior was observed in the nucleation and crystallization of ice (27). In the above systems, nucleation may be expected to be homogeneous. While the nucleation characteristics of mannitol in the mannitol-trehalose-water system can be explained by the theory of homogeneous nucleation, it is recognized that in presence of ice, the secondary crystallization of mannitol is likely to be heterogeneous.

The above results bring to light the combined effects of thermodynamics and kinetics on the crystallization of solutes in frozen solution. Crystallization of mannitol (10% w/w) appears to have been prevented in presence of trehalose (5% w/w) only below Tg'_1 . Next, we studied frozen aqueous solutions of mannitol (10% w/w) in presence of a lower trehalose concentration (2% w/w). When these solutions were annealed below the transition temperatures, the enthalpy of crystallization decreased as a function of the annealing time (Fig. 7, curve b). This indicated that mannitol crystallized during isothermal annealing as was observed in the absence of trehalose (Fig. 2). Therefore, the trehalose concentration was not high enough to delay the crystallization of mannitol. When the

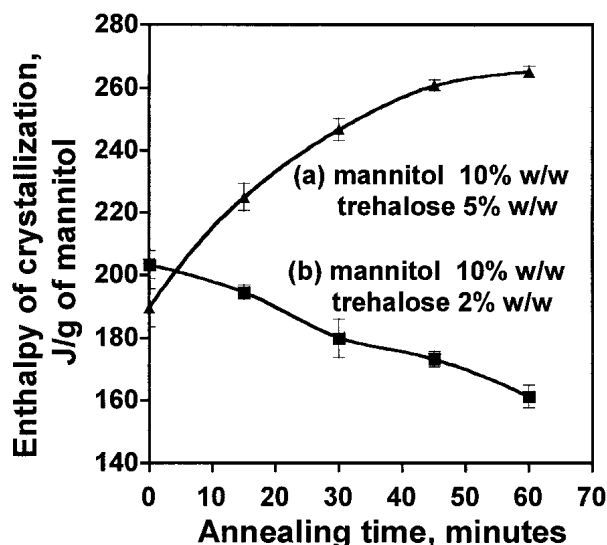


Fig. 7. The effect of trehalose concentration on the crystallization behavior of mannitol following sub- Tg'_1 annealing. Frozen solutions were annealed at 4°C below their respective Tg'_1 values of -41°C (5% w/w trehalose) and -35°C (2% w/w trehalose). Each point is the mean of three determinations. Error bars represent standard deviations ($n = 3$).

trehalose concentration was increased to 5% (w/w), there was only nucleation during annealing whereas the crystallization appeared to be completely inhibited (Fig. 7, curve a). At longer annealing times, the enthalpy of crystallization was higher, indicating an increase in the number of nuclei formed. It must be pointed out that because the crystallization exotherm overlapped with the ice melting endotherm, the absolute enthalpy values are not deemed to be reliable. Our conclusions are based on the observed trend.

Transitions during Primary Drying

By attaching a vacuum pump to the low-temperature stage, the entire freeze-drying cycle was simulated in the sample chamber of the X-ray diffractometer. Aqueous solutions of mannitol (10% w/w) alone or in combination with trehalose (5% w/w) were freeze-dried and the phases were monitored. In case of solutions containing only mannitol, the solutions were cooled at $20^\circ\text{C}/\text{min}$ to -70°C , held for 20 min, and heated to the primary drying temperature of -35°C at $5^\circ\text{C}/\text{min}$. The crystallization of mannitol hydrate was evident soon after the primary drying was initiated (data not shown). When trehalose was present, the solutions were cooled to -70°C at $1^\circ\text{C}/\text{min}$, held for 15 min, and heated to -41°C at $5^\circ\text{C}/\text{min}$ where primary drying was carried out. The characteristic peaks of mannitol hydrate appeared after 20 min of primary drying (Fig. 8). During the initial stages of primary drying, there was a pronounced increase in the peak intensity as a function of drying time. However, a substantial fraction of the solute was retained amorphous, even at the end of primary drying. Secondary drying at -10°C did not cause any pronounced changes in the solid state of the solute. Because trehalose did not crystallize, all the observed peaks could be attributed to mannitol.

Mannitol, in the absence of trehalose, crystallized rapidly during primary drying. In presence of trehalose, the crystal-

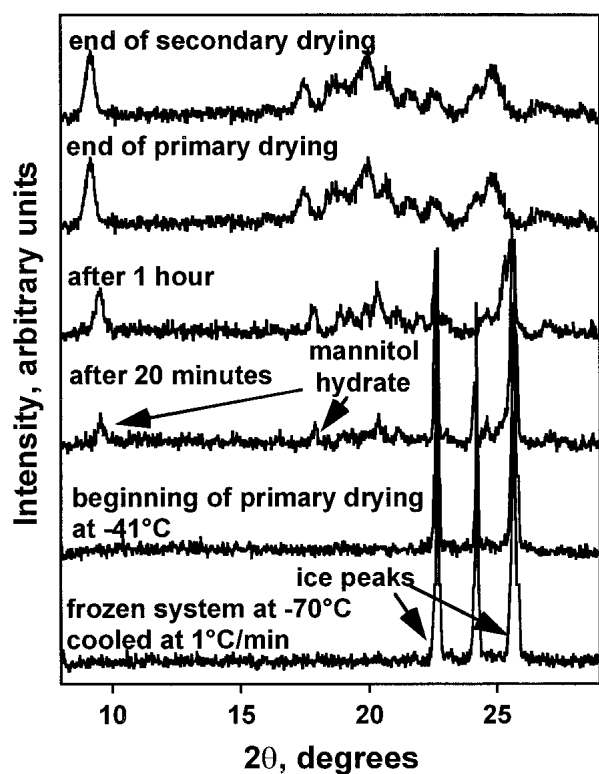


Fig. 8. *In situ* XRD during freeze-drying of aqueous solution of mannitol (10% w/w) and trehalose (5% w/w). The solution was cooled from room temperature to -70°C at $1^{\circ}\text{C}/\text{min}$ and then heated to the primary drying temperature of -41°C at $5^{\circ}\text{C}/\text{min}$. Primary drying was conducted for ~ 8 h, following which it was heated to -10°C where secondary drying was carried out for ~ 2 h.

lization of mannitol was slightly delayed. When solutions containing mannitol and trehalose were rapidly cooled ($20^{\circ}\text{C}/\text{min}$), crystallization was observed only during secondary drying. While slower cooling rates may facilitate nucleation and therefore crystallization below glass transition, nucleation may not occur in rapidly cooled solutions.

Significance

Conventionally, solid-state and physical characterization studies have been restricted to the final freeze-dried product. This does not provide information about physical changes (glass transition, crystallization, and solid-state transition) during the various stages of the freeze-drying process. We have investigated the crystallization behavior of mannitol in presence and in absence of trehalose during the various stages of the freeze-drying process. When freeze-dried alone, mannitol is not retained amorphous. If it does not crystallize during cooling, it will crystallize during primary drying. The presence of a noncrystallizing excipient, in this case trehalose, affected the crystallization behavior of mannitol. It is known that mannitol is retained amorphous in the freeze-dried state only when its concentration in the final freeze-dried product is less than 30% (w/w) and the other component(s) are noncrystallizing. In our lyophilized systems, the final mannitol concentration was at least 67% (w/w). At such high concentrations, crystallization of mannitol was delayed but not prevented.

During the cooling stage, ice crystallization may be in-

hibited. Even if the system is supersaturated with respect to mannitol, the degree of supersaturation will not be high. Annealing below T_g' facilitated ice crystallization, resulting in a highly supersaturated mannitol solution. At a lower trehalose concentration (2% w/w), nucleation as well as crystallization of mannitol occurred during sub- T_g' annealing. However, at a higher trehalose concentration, mannitol crystallized only during the drying stage.

The crystallization of mannitol below the glass transition temperature is possibly a reflection of its high molecular mobility. The inhibitory effect of trehalose on its crystallization can be understood by considering both thermodynamics and kinetic factors. The presence of an additive may prevent attainment of supersaturation. In such cases, the system is under thermodynamic control. As pointed out by Rodriguez-Hornedo and Murphy (22), this may often be erroneously attributed to the inhibition of nucleation by the additive. Our results show that sub- T_g' annealing in mannitol-trehalose systems led to ice crystallization followed by attainment of supersaturation and then nucleation. This supports the hypothesis that there was an unsaturated state prior to annealing. However, mannitol did not crystallize below the glass transition temperature of the amorphous freeze-concentrate in presence of trehalose in the time-scales studied. It is possible that kinetic factors, such as high viscosity and reduced molecular mobility, control the process.

Annealing below the glass transition temperature usually results in enthalpic relaxation due to the existence of molecular mobility (28,29). In systems containing only mannitol, because the solute crystallized below T_g' the issue of enthalpic relaxation is irrelevant. In presence of trehalose (at $\geq 5\%$ w/w), while mannitol crystallization was inhibited, the molecular mobility was evident from the enthalpic recovery associated with the T_g' (Figs. 5 and 6a). This observation also reveals that the molecular mobility of mannitol is reduced in presence of trehalose.

There are some interesting parallels between our investigation and aging studies on vitrified solutions. In these highly concentrated vitrified systems reported in the literature (19,23,30), complete ice crystallization did not occur during cooling. Sub- T_g' annealing led to an increase in the density of ice nuclei that crystallized on heating (23). The formation of ice in these systems is described in the literature as "devitrification." The number of ice nuclei increased at longer annealing times, resulting in a decrease in the temperature of devitrification. In the mannitol-trehalose system, at all trehalose concentrations investigated, mannitol did not crystallize during cooling. Sub- T_g' annealing led to ice crystallization followed by mannitol nucleation. While there is clear evidence of nucleation of mannitol below the glass transition temperature of the amorphous freeze-concentrate, the temperature of its crystallization is a function of trehalose concentration.

CONCLUSIONS

In frozen aqueous solutions of mannitol (10% w/w), the solute crystallized below T_g' . The addition of trehalose at low concentration (2% w/w) did not significantly alter the crystallization behavior of mannitol. When the trehalose concentration was high (5% w/w), mannitol did not crystallize below the observed glass transition temperatures. Sub- T_g' annealing

led to ice crystallization, thus facilitating the attainment of supersaturation. This was followed by nucleation of mannitol during annealing. The crystallization behavior of mannitol in presence of trehalose was also dependent on the annealing temperature, time, and heating rate. XRD revealed mannitol crystallization during primary drying below the T_g' both in presence and in absence of trehalose. *In situ* XRD was an excellent complement to DSC in the characterization of frozen aqueous solutions of mannitol.

ACKNOWLEDGMENTS

Partial financial support from the Parenteral Drug Association Foundation for Pharmaceutical Sciences and from the International Student Work Opportunity Program, University of Minnesota, is greatly appreciated. We thank Dr. Evgenyi Shalaev for his valuable comments.

REFERENCES

1. A. I. Kim, M. J. Akers, and S. L. Nail. The physical state of mannitol after freeze-drying: Effects of mannitol concentration, freezing rate, and a noncrystallizing cosolute. *J. Pharm. Sci.* **87**:931–935 (1998).
2. K. Izutsu, S. Yoshioka, and T. Terao. Effect of mannitol crystallinity on the stabilization of enzymes during freeze-drying. *Chem. Pharm. Bull.* **42**:5–8 (1994).
3. L. Yu. D. S. Mishra, and D. R. Rigsbee. Determination of the glass properties of D-mannitol using sorbitol as an impurity. *J. Pharm. Sci.* **87**:774–777 (1998).
4. N. A. Williams and T. Dean. Vial breakage by frozen mannitol solutions: Correlation with thermal characteristics and effect of stereoisomerism, additives, and vial configuration. *J. Parenter. Sci. Technol.* **45**:94–100 (1991).
5. N. A. Williams, Y. Lee, G. P. Polli, and T. A. Jennings. The effects of cooling rate on solid phase transitions and associated vial breakage occurring in frozen mannitol solutions. *J. Parenter. Sci. Technol.* **40**:135–141 (1986).
6. A. Martini, S. Kume, M. Crivellente, and R. Artico. Use of sub-ambient differential scanning calorimetry to monitor the frozen-state behavior of blends of excipients for freeze-drying. *PDA J. Pharm. Sci. Technol.* **51**:62–67 (1997).
7. R. K. Cavatur and R. Suryanarayanan. Characterization of phase transitions during freeze-drying by *in situ* X-ray powder diffraction. *Pharm. Dev. Technol.* **3**:579–586 (1998).
8. J. F. Carpenter and B. S. Chang. Lyophilization of protein pharmaceuticals. In K. E. Avis and V. L. Wu (eds.), *Biotechnology and Biopharmaceutical Manufacturing, Processing and Preservation*, Interpharm Press, Buffalo Grove, Illinois, 1996, pp. 199–264.
9. R. K. Cavatur and R. Suryanarayanan. Characterization of frozen aqueous solutions by low temperature X-ray powder diffractometry. *Pharm. Res.* **15**:194–199 (1998).
10. J. F. Carpenter, K.-I. Izutsu, and T. W. Randolph. Freezing- and drying-induced perturbations of protein structure and mechanisms of protein protection by stabilizing additives. *Drugs Pharm. Sci.* **96**:123–160 (1999).
11. W. Wang. Lyophilization and development of solid protein pharmaceuticals. *Int. J. Pharm.* **203**:1–60 (2000).
12. B. D. Herman, B. D. Sinclair, N. Milton, and S. L. Nail. The effect of bulking agent on the solid-state stability of freeze-dried methylprednisolone sodium succinate. *Pharm. Res.* **11**:1467–1473 (1994).
13. L. Yu. N. Milton, E. G. Groleau, D. S. Mishra, and R. E. Vansickle. Existence of a mannitol hydrate during freeze-drying and practical implications. *J. Pharm. Sci.* **88**:196–198 (1999).
14. R. K. Cavatur, N. M. Vemuri, A. Pyne, Z. Chrzan, D. Toledo-Velasquez, and R. Suryanarayanan. Crystallization behavior of mannitol in frozen aqueous solutions. *Pharm. Res.* **19**:894–900 (2002).
15. M. Yoshioka, B. C. Hancock, and G. Zografi. Crystallization of indomethacin from the amorphous state below and above its glass transition temperature. *J. Pharm. Sci.* **83**:1700–1705 (1994).
16. A. Burger, J.-O. Henck, S. Hetz, J. M. Rollinger, A. A. Weissnicht, and H. Stottner. Energy/temperature diagram and compression behavior of the polymorphs of D-mannitol. *J. Pharm. Sci.* **89**:457–468 (2000).
17. E. Y. Shalaev and F. Franks. Structural glass transitions and thermophysical processes in amorphous carbohydrates and their super-saturated solutions. *J. Chem. Soc. Faraday Trans.* **91**:1511–1517 (1995).
18. L. Chang, X. Tang, M. J. Pikal, N. Milton, and L. Thomas. The origin of multiple glass transitions in frozen aqueous solutions. *Proc. NATAS Annu. Conf. Therm. Anal. Appl.* **27**:624–628 (1999).
19. S. Ablett, M. J. Izzard, and P. J. Lillford. Differential scanning calorimetric study of frozen sucrose and glycerol solutions. *J. Chem. Soc. Faraday Trans.* **88**:789–794 (1992).
20. H. R. Costantino, J. D. Andya, P.-A. Nguyen, N. Dasovich, T. D. Sweeney, S. J. Shire, C. C. Hsu, and Y.-F. Maa. Effect of mannitol crystallization on the stability and aerosol performance of a spray-dried pharmaceutical protein, recombinant humanized anti-IgE monoclonal antibody. *J. Pharm. Sci.* **87**:1406–1411 (1998).
21. J. W. Mullin. *Crystallization*, 2nd edition, Butterworth Heinemann, London, 1972.
22. N. Rodriguez-Hornedo and D. Murphy. Significance of controlling crystallization mechanisms and kinetics in pharmaceutical systems. *J. Pharm. Sci.* **88**:651–660 (1999).
23. Z. Chang and J. G. Baust. Physical aging of the glassy state: Sub- T_g ice nucleation in aqueous sorbitol solutions. *J. Non-Cryst. Solids* **130**:198–203 (1991).
24. A. Pyne, R. Surana, and R. Suryanarayanan. Enthalpic relaxation in frozen aqueous solutions using differential scanning calorimetry. *AAPS PharmSci* **3**:1522–0893 (2001).
25. J. W. Mullin and C. L. Leci. Nucleation characteristics of aqueous citric acid solutions. *J. Cryst. Growth* **5**:75–76 (1969).
26. D. Turnbull and J. C. Fisher. Rate of nucleation in condensed systems. *J. Chem. Phys.* **17**:71–73 (1949).
27. F. Franks, S. F. Mathias, and K. Trafford. The nucleation of ice in undercooled water and aqueous polymer solutions. *Colloids Surf.* **11**:275–285 (1984).
28. B. C. Hancock, S. L. Shamblin, and G. Zografi. Molecular mobility of amorphous pharmaceutical solids below their glass transition temperatures. *Pharm. Res.* **12**:799–806 (1995).
29. L. C. E. Struik. *Physical Aging in Amorphous Polymers and Other Materials*, Elsevier Scientific Publishing Company, New York, 1978.
30. Z. Chang and J. G. Baust. Further inquiry into the cryobehavior of aqueous solutions of glycerol. *Cryobiology* **28**:268–278 (1991).